

Electronic transport properties of giant-magnetoresistance Fe/Cr multilayers

M. Jacob, G. Reiss,* H. Brückl, and H. Hoffmann

Institut für Angewandte Physik III, Universität Regensburg, Universitätsstrasse 31, D-8400 Regensburg, Germany

(Received 22 July 1992)

Thin Fe/Cr multilayered films are the most intensively investigated system with regard to the recently discovered giant magnetoresistance (GMR). In order to contribute to the understanding of this effect, we present the results of resistance measurements during growth of Fe/Cr single-layer and multilayer films. We determined the transport parameters of these films and compared the thickness dependent conductances of ferromagnetic and antiferromagnetic coupled layers. The difference in the conductances shows complete saturation for Fe thicknesses above 3 nm and is consistent with the *ex situ* measured GMR of the antiferromagnetic film. This points to interface scattering as origin of the GMR. With respect to this result we investigated the influence of the interface roughness on the amount of GMR.

INTRODUCTION

The reasons for the intensive investigations of Fe/Cr multilayers are properties attributed to the layered structure. First an antiparallel alignment of the magnetizations of successive Fe layers has been found.¹ The second important discovery was the giant magnetoresistance (GMR).^{2,3} An external field orients the magnetic moments of the Fe layers parallelly; this lowers the electrical resistivity by almost a factor 2 at 4 K. Third Parkin *et al.* found the oscillating behavior of the interlayer exchange coupling;⁴ They reported antiferromagnetic (AF) coupling for Cr thicknesses of about 1 nm and ferromagnetic (FM) coupling for thicknesses of about 1.8 nm.

The reason for the additional electron scattering in the AF state and thereby for the very large resistivity change (GMR) has not been satisfactorily understood. Camley and Barnaś developed a semiclassical approach to describe the GMR.^{5,6} They calculated the resistivity by solving the Boltzmann transport equation. Bulk and interface scattering are expressed phenomenologically by introducing spin-dependent mean free paths and boundary conditions with spin-dependent transmission coefficients. Levy and co-workers established a quantum model with spin-dependent scattering potentials in order to express the interface and bulk scatterings.^{7,8}

In order to obtain numerical results, both groups had to use some unknown parameters; two are the intrinsic mean free paths (IMFP) and the resistivities of iron and chromium. In addition, the calculations of Barnaś *et al.* for sandwich structures involve the specular parameter p , which was introduced first by Fuchs.⁹ In a number of previous publications,¹⁰ we discussed an experimental method for a quantitative determination of these parameters in thin films.

Since the bulk as well as the interface scattering can be spin dependent and contribute to the GMR, investigations of the electronic transport mechanism are necessary. The enhancement of resistance by spin-dependent electron scattering is expected to appear already during

the growth of the films. Therefore *in situ* resistance measurements are a suitable tool to locate the GMR effect. Finally we investigated the influence of both the mesoscopic and the microscopic interface roughness on the magnitude of the GMR.

EXPERIMENTS AND STRUCTURAL SAMPLE CHARACTERIZATION

The samples used for this study were evaporated in UHV with a rate of 0.2, . . . , 0.3 nm/sec onto fire-polished corning glass, held at 300 K. During the evaporation the film thickness was controlled by a quartz oscillator; the resistance was measured by a spring-loaded four point probe with gold tips.

Figure 1 shows a scanning-tunneling-microscopy (STM) image of the surface of a $[\text{Fe}(3.0 \text{ nm})/\text{Cr}(0.9 \text{ nm})]_2/\text{Fe}(3.0 \text{ nm})/\text{Au}(2.0 \text{ nm})$ film. The amplitude of the topological fluctuations of the surface is smaller than 2 nm.

A number of films was examined by TEM. The micrographs show polycrystalline structures with columns grown vertically through the whole multilayer (60 nm). Laterally the grain diameters are 10–20 nm, corresponding to the STM images of the film surfaces (Fig. 1). At certain sites we could find continuous layered structures

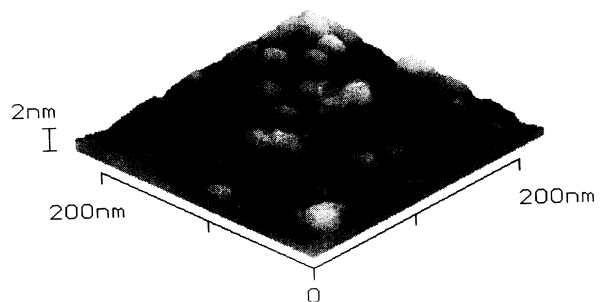


FIG. 1. STM image of a structure of the form $\text{Fe}(3.0 \text{ nm})/[\text{Cr}(0.9 \text{ nm})/\text{Fe}(3.0 \text{ nm})]_2/\text{Au}(2.0 \text{ nm})$.

within the grains. This is presumably due to the similarities in crystal lattice (both bcc) and lattice constants of Fe and Cr and points to the presence of a fibertexture in the films. The purity of the samples was tested by Auger sputter depth profiling.

RESULTS AND DISCUSSION

Transport parameters

Transport parameters were determined from the thickness dependence of the resistivity of single Fe and Cr films. Figure 2 shows a plot of the product ρt (resistivity times film thickness) versus t of a single Fe film. For the evaluation of the transport parameters, we fitted the Fuchs-Namba theory^{9,11} to the experimental data by varying the four parameters ρ_∞ (bulk resistivity), l_∞ (IMFP), p (specularity parameter), and H (mesoscopic surface roughness). Since the separation of p and l_∞ is problematical, we give the value of the product $l_\infty(1-p)$ in Table I. From covering experiments we obtained the information that $p \approx 0$ and thereby $l_\infty \gtrsim 10$ nm for both materials.

These transport parameters can be introduced in the interpretation of the GMR. Although the mesoscopic surface roughness H of these single-layer films differs from the surface and interface roughnesses of multilayered systems, the other values should keep the same. The most interesting parameters are the IMFP (l_∞) of Fe and Cr. These scattering lengths are essential for the electronic transport properties in these films. In our investigation they turn out to be considerably larger than the layer thickness of typical Fe/Cr multilayered films. Therefore, one important precondition for the occurrence of the GMR is fulfilled.

Ex situ measured GMR

We define the longitudinal change of the GMR ratio (e.g., the magnetic field H parallel to the current) of samples with AF coupling as

$$\frac{\Delta R}{R} = \frac{R^{\uparrow\downarrow} - R^{\uparrow\uparrow}}{R^{\uparrow\uparrow}} \quad (1)$$

with $R^{\uparrow\downarrow}$ the maximum value of $R(H)$ corresponding to antiparallel alignment of the magnetizations of successive Fe-layers and $R^{\uparrow\uparrow}$ the minimum value of $R(H)$ (parallel alignment). A series of multilayers with varying thick-

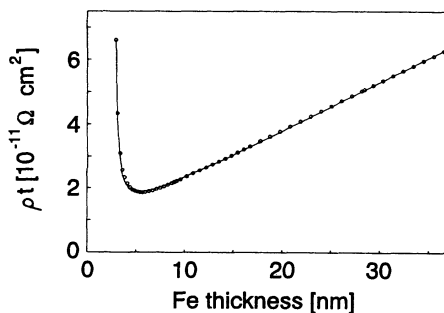


FIG. 2. Experimental (circles) and theoretical (line) results for the resistivity ρ times film thickness t vs t of a Fe monolayer.

TABLE I. Transport parameters of Fe and Cr, achieved by fits on five Fe and three Cr monolayers.

	ρ_∞ ($\mu\Omega$ cm)	$l_\infty(1-p)$ (nm)	H (nm)
Fe	16 ± 2	11 ± 1	$2,5 \pm 0,2$
Cr	32 ± 1	10 ± 1	$2,2 \pm 0,7$

ness of Cr at constant Fe thickness (3.6 nm), showed the expected oscillations of the GMR with 1.8 ± 0.3 nm periodicity as reported by Parkin, More and Roche.⁴ Vibrating-sample magnetometer (VSM) measurements confirmed the presence and the absence of AF coupling according to the Cr thickness as reported.^{4,12,13}

The values of the GMR ratio are consistent with previously reported data with respect to temperature (300 K) and number of bilayers (3).^{2,3,14,15} A sample with 30 [Fe(1.2 nm)/Cr(1.0 nm)] bilayers showed an effect of 55% at 4 K.

In situ measurements on multilayers

In order to obtain quantitative experimental results on the development of GMR with the increasing Fe thickness we carried out resistance measurements during the deposition of the Fe/Cr multilayers. Since a magnetic field necessary for the magnetic saturation of the samples was not available during the evaporation, we used the fact that samples with Cr thickness of about 1 nm and 2 nm are AF and FM coupled, respectively. Therefore, it should be possible to obtain the thickness dependence of the GMR by comparing the *in situ* measured resistance versus t_{Fe} curves.

Because of our interest in extracting the development of the GMR during the deposition of one of the Fe layers we had to become independent of the base conductance (see Fig. 3). We applied a model of parallel resistors with the base resistance R_b :

$$G_{Fe} = 1/R_{Fe} = 1/R - 1/R_b \quad (2)$$

This was done for single Fe-layers of a sample with FM coupling and for the corresponding single Fe layers of a sample with AF coupling. The conductance $G_{Fe}^{\uparrow\uparrow}$ of the FM-coupled layer depends on the layer thickness as

$$G_{Fe}^{\uparrow\uparrow}(t_{Fe}) \propto 1/\rho_\infty f(t_{Fe})t_{Fe} \quad (3)$$

where $f(t_{Fe})$ represents the thickness dependence of the

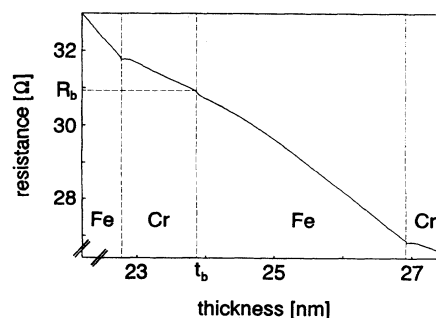


FIG. 3. Section of *in situ* measurement on a multilayer: resistance vs film thickness for the 6 Cr layer (22.8–23.9 nm) and the 7 Fe layer (23.9–26.9 nm).

conductivity. The GMR effect enhances the resistance of the AF-coupled Fe layer, which otherwise shows a similar behavior.

In Fig. 4(a), the two conductance curves for the fourth Fe layers are shown. The subtraction of the two different conductances $\Delta G_{Fe}(t_{Fe}) = G_{Fe}^{\uparrow\uparrow}(t_{Fe}) - G_{Fe}^{\uparrow\downarrow}(t_{Fe})$ gives the dependence of the additional spin-dependent scattering of the conduction electrons on the Fe layer thickness [Fig. 4(b)]. As can be seen in Fig. 4(a), the conductances of the AF and FM coupled sample show a linear dependence on t_{Fe} for thicknesses larger than 3 nm. The application of the Fuchs theory⁹ with different specularly parameters p_{FM}, p_{AF} for the different Fe layers leads to the same behavior. For thicknesses smaller than 3 nm the behavior of $\Delta G_{Fe}(t_{Fe})$ [Fig. 4(b)] is different for different pairs of Fe layers. Sometimes there is a small maximum as shown in Fig. 4(b); sometimes $\Delta G_{Fe}(t_{Fe}) = \text{const}$ already after the sharp kink at $t_{Fe} = 1$ nm. We attribute these differences to structural effects. The maximum in Fig. 4(b), for example, can be explained by slightly different roughnesses of the interfaces of the two films. The common feature of all curves, however, is the sharp kink at $t_{Fe} \approx 1$ nm and the saturation below 3 nm.

The main problem of this proceeding is to grow the films under exactly the same conditions. Only for this case the values for ρ_{∞} are comparable to each other. To check the results, we added up the values of $\Delta G_{Fe}(t_{Fe} > 3 \text{ nm})$ of every Fe layer of a whole film and divided by the conductance $G^{\uparrow\downarrow}$ of the AF-coupled sample. Applying a model of parallel resistors to the conductances of the single layers yields the GMR ratio

$$\frac{\Delta R}{R} = \sum_{i=1}^n \frac{\Delta G_{Fe,i}(t_{Fe} > 3 \text{ nm})}{G^{\uparrow\downarrow}}$$

for $n = \text{number of bilayers}$. (4)

The comparison with *ex situ* measured GMR agrees within 15% tolerance. This demonstrates, that the evaluation of ΔG yields the additional scattering of the electrons in the Af film due to the GMR.

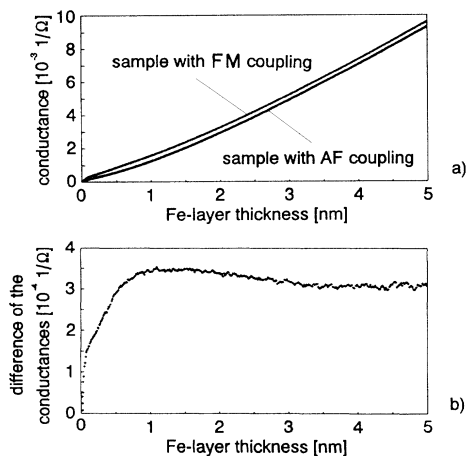


FIG. 4. (a) Conductances of two extracted corresponding Fe layers, one FM coupled and one AF coupled. (b) The development of the GMR ratio during the growth of one of the Fe layers of the AF coupled sample.

Diény¹⁶ recently reported his calculations of ΔG for spin-dependent bulk and interface scattering of the electrons as reason for the GMR. He thereby applied the model of Camley and Barnaš and co-workers,^{5,6} the result was a saturation of ΔG in both cases. For interface scattering, however, ΔG reaches saturation at lower values of t_{Fe} than for bulk scattering. Our investigation shows a saturation of ΔG at $t_{Fe} \approx 3$ nm. Therefore, this result strongly points to interface scattering as the dominant mechanism responsible for the GMR.

Influence of interface roughness

With respect to the confirmation that GMR is an interface effect it is interesting to investigate the influence of the interface roughness on the amount of GMR. First we varied only the mesoscopic roughness H . A small amount of Au grows on glass in the form of islands.¹⁷ We assume that covering Fe/Cr-layers tend to keep this additional roughness (Fig. 5). This was confirmed by *ex situ* STM imaging of the films.

We produced three samples of the structure $\text{Au}(x \text{ nm})/[\text{Fe}(3.0 \text{ nm})/\text{Cr}(0.9 \text{ nm})]_2/\text{Fe}(3.0 \text{ nm})/\text{Au}(2.0 \text{ nm})$ (with $x = 0.0/1.0/2.0$ nm). STM images allowed us to determine the mean mesoscopic surface roughness. The method is described elsewhere.^{18,19} We assumed that, similar to the case of Au on Ni,¹⁹ the covering Au layer does not change the roughness essentially in the nm range. Figure 6 shows the MR ratio versus the measured mesoscopic surface roughness. The GMR effect decreases drastically with increasing roughness. An additional roughness of about 0.8 nm decreases the GMR by a factor of 5. It is obvious that the AF alignment of the magnetization of successive Fe layers becomes very improbable in these structures.

As a second attempt to investigate the influence of the interface structures on the GMR, we introduced additional mixing regions similar to the idea of Petroff *et al.*²⁰ We produced a series of samples of the form $\text{Cr}(3.0 \text{ nm})/[\text{Fe}(3.0 \text{ nm})/\text{Cr}(1.1 \text{ nm})]_3/\text{Fe}(3.0 \text{ nm})/\text{Au}(2.0 \text{ nm})$. Between the periods of evaporation of Fe and Cr we inserted periods, in which we evaporated both materials simultaneously with the same rate. The amount of evaporated material is the same for every sample. The film resistance increases with increasing thickness of the mixed layer as shown in Fig. 7(a). This is due to the addition of scattering centers by the increasing layer mixing. The behavior of the GMR [Fig. 7(b)] is remarkable: Up to 0.5-nm thickness of the mixed area the MR ratio does not show any essential change. We had to enhance this area nearly to 0.9 nm in order to diminish remarkably the

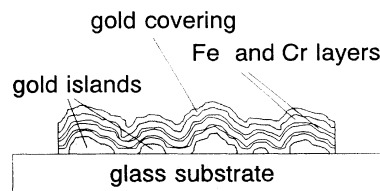


FIG. 5. Sketch of a multilayer, grown on a glass substrate covered with gold islands.

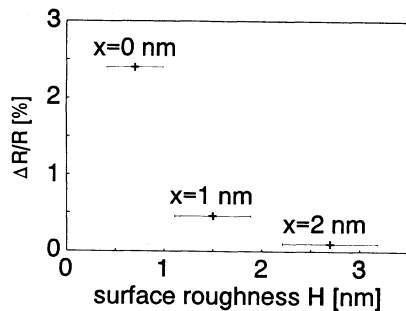


FIG. 6. MR ratio vs mesoscopic surface roughness. It is assumed that the interface roughness is similar to the surface roughness. The relative small GMR values are attributed to the small number of only two bilayers.

GMR ($\Delta R/R = 0.7\%$). Thereby the saturation field H_S , which remained constant for the samples with mixed areas thinner than 0.5 nm, was reduced by a factor of 4. The reduction of the GMR in these samples was confirmed by VSM measurements to be accompanied by a breakdown of the AF coupling.

The results of our experiments differ from the results of Petroff *et al.*²⁰ They reported an enhancement of the MR ratio by a mixed area thickness of 0.1 nm and a strong decrease at 0.4 nm. We attribute the different results to the difference of the samples. It seems that the molecular-beam-epitaxy-grown films of Petroff *et al.* have a smaller original roughness of the interfaces than our evaporated, polycrystalline samples.

CONCLUSIONS

To summarize we determined the transport properties of Fe and Cr and applied *in situ* measurements of the resistance in order to obtain a quantitative information about the location of the spin-dependent electron scattering. The additional scattering of the conduction electrons in AF samples occurs within a 1–3 nm-thick region at the Fe/Cr interfaces. Thus the interface scattering

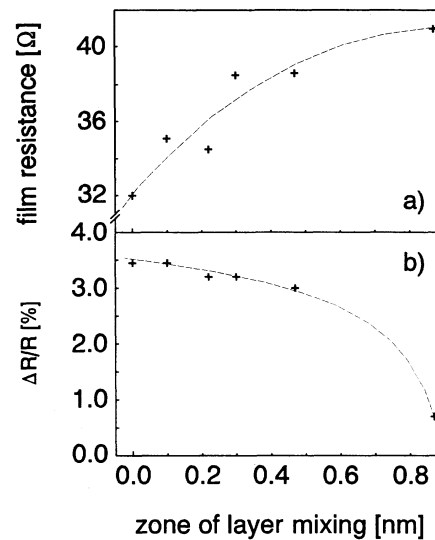


FIG. 7. Variation of the interface microstructure. x axis: thickness of the artificially added mixing region of Fe and Cr. (a) Film resistance and (b) GMR ratio.

seems to be the dominating reason for the GMR in these samples. Furthermore, we found the following influence of the interface roughness on the GMR: If only the roughness of these polycrystalline samples is enhanced, the GMR-ratio decreases. The dependence on the mesoscopic roughness is strong, presumably due to the suppression of the AF coupling when the roughness becomes comparable to the layer thickness. On the other hand, the dependence on the thickness of mixing regions at the interfaces is weak within a range of 0.5 nm. The decrease of the GMR for mixing region thicker than 0.8 nm is accompanied by a breakdown of the AF coupling. Further efforts concerning a quantitative analysis of GMR by application of existing theories^{5–8} to films with well-known transport parameters and the application of the presented methods to the Co/Cu system are in progress.²¹

*Present address: IBM Thomas J. Watson Research Center, Yorktown Heights, NY 10598.

¹P. Grünberg, R. Schreiber, Y. Pang, M. B. Brodsky, and H. Sowers, *Phys. Rev. Lett.* **57**, 2442 (1986).

²M. N. Baibich, J. M. Broto, A. Fert, F. Nguyen Van Dau, and F. Petroff, *Phys. Rev. Lett.* **61**, 2472 (1988).

³G. Binasch, P. Grünberg, F. Saurenbach, and W. Zinn, *Phys. Rev. B* **39**, 4828 (1989).

⁴S. S. P. Parkin, N. More, and K. P. Roche, *Phys. Rev. Lett.* **64**, 2304 (1990).

⁵R. E. Camley and J. Barnaś, *Phys. Rev. Lett.* **63**, 664 (1989).

⁶J. Barnaś, A. Fuss, R. E. Camley, P. Grünberg, and W. Zinn, *Phys. Rev. B* **42**, 8110 (1990).

⁷P. M. Levy, S. Zhang, and A. Fert, *Phys. Rev. Lett.* **65**, 1643 (1990).

⁸P. M. Levy, K. Ounadjela, S. Zhang, Y. Wang, C. B. Sommers, and A. Fert, *J. Appl. Phys.* **67**, 5914 (1990).

⁹K. Fuchs, *Proc. Camb. Philos. Soc.* **34**, 100 (1938).

¹⁰J. Vancea, G. Reiss, and H. Hoffmann, *Phys. Rev. B* **35**, 6435 (1987); G. Reiss, K. Kapfberger, G. Meier, J. Vancea, and H. Hoffmann, *J. Phys. Condens. Matter* **1**, 1275 (1989); U.

Jacob, J. Vancea, and H. Hoffmann, *Phys. Rev. B* **41**, 11 852 (1990).

¹¹Y. Namba, *Jpn. J. Appl. Phys.* **9**, 1326 (1970).

¹²P. Grünberg, S. Demokritov, A. Fuss, M. Vohl, and J. A. Wolf, *J. Appl. Phys.* **69**, 4789 (1991).

¹³M. Donath, D. Scholl, D. Mauri, and E. Kay, *Phys. Rev. B* **43**, 13 164 (1991).

¹⁴S. Araki and T. Shinjo, *Jpn. J. Appl. Phys.* **29**, 621 (1990).

¹⁵P. Grünberg, J. Barnaś, F. Saurenbach, J. A. Fuss, A. Wolf, and M. Vohl, *J. Magn. Magn. Mater.* **93**, 58 (1991).

¹⁶B. Dieny (unpublished).

¹⁷L. Reimer and K. Freking, *Z. Phys.* **184**, 119 (1965).

¹⁸G. Reiss, H. Brückel, J. Vancea, R. Lecheler, and E. Hastreiter, *J. Appl. Phys.* **70**, 523 (1991).

¹⁹G. Reiss, E. Hastreiter, H. Brückel, and J. Vancea, *Phys. Rev. B* **43**, 5176 (1991).

²⁰F. Petroff, A. Barthélémy, A. Hamzić, A. Fert, P. Etienne, S. Lequien, and G. Creuzet, *J. Magn. Magn. Mater.* **93**, 95 (1991).

²¹M. Jacob, T. Eckl, G. Reiss, and H. Hoffmann (unpublished).

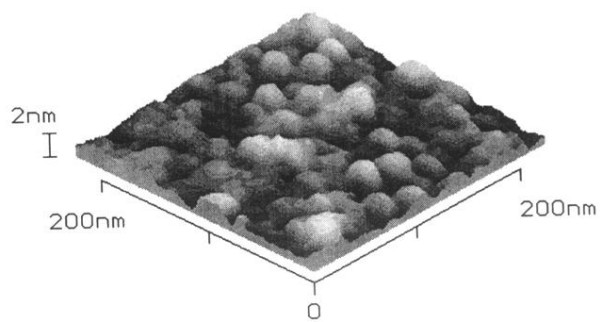


FIG. 1. STM image of a structure of the form $\text{Fe}(3.0 \text{ nm})/[\text{Cr}(0.9 \text{ nm})/\text{Fe}(3.0 \text{ nm})]_2/\text{Au}(2.0 \text{ nm})$.

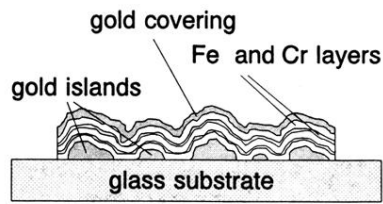


FIG. 5. Sketch of a multilayer, grown on a glass substrate covered with gold islands.